

# Beam parameters of a Möbius ring

V. Ziemann, FREIA, Uppsala University

January 5, 2022

## Abstract

We describe a racetrack-shaped ring in which the cross-plane coupling can be continuously varied between an uncoupled configuration to a Möbius configuration, where the transverse planes change role after one turn. Tunes, emittances, and other beam parameters that depend on the emission of synchrotron radiation are calculated as a function of the coupling.

## 1 Introduction

In order to explore a new algorithm [1] to calculate the radiation integrals [2] we designed an accelerator lattice for a storage ring in which the transverse coupling can be continuously varied; all the way from the uncoupled lattice to a Möbius configuration [3] and even beyond. Then we calculate the radiation integrals for this strongly coupled lattice and derive beam parameters such as the emittances.

All MATLAB scripts used to design this ring are available from [4]. The software is based on [5] but is adapted to handle coupling and dispersion effects simultaneously. In order to keep the design conceptually simple, we use thin-lens quadrupoles, both for the upright and the skew quadrupoles and base our design on the  $90^\circ$  FODO cell, shown on the left-hand side in Figure 1. This cell has a length of  $2L = 10$  m, where  $L = 5$  m is the length of the drift space between the quadrupoles, which have a focal length of  $L/\sqrt{2}$ , giving the phase-advance of 90 degrees per cell in both planes. The beta functions assume their maximum and minimum value of 17.7 and 2.9 m, respectively. The value in the middle of the straight section is  $3L/2 = 7.5$  m.

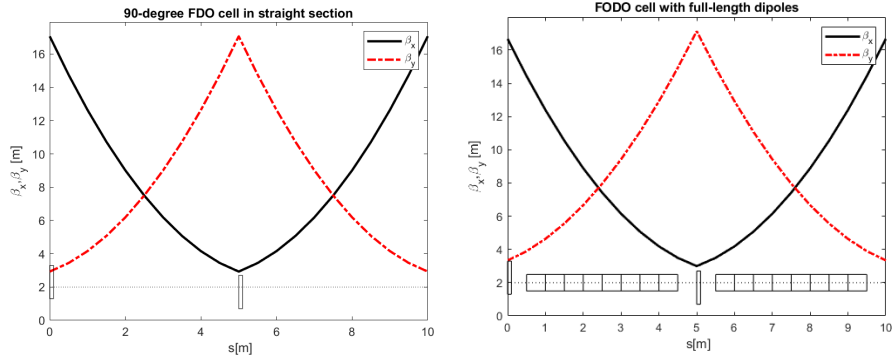


Figure 1: The beta function of the basic 90-degree cell (left) and a cell with 4 m-long dipoles used in the arcs (right).

In the arcs we insert 4 m long dipoles with a deflection angle of 2 degrees in each of the straight sections between the quadrupoles. The right-hand side in Figure 1 illustrates this. In order to avoid equal integer tunes in both planes we adjust the quadrupoles in these cells to give phase advances of  $0.25 \times 360^\circ$  and  $0.22 \times 360^\circ$  in the horizontal and vertical plane, respectively.

## 2 Arcs

Each of the two arcs consist of 43 standard cells shown on the right-hand side in Figure 1 and two cells with half-length dipoles each on either end. These additional cells create an interference pattern in the periodically oscillating dispersion that cancels the dispersion almost perfectly. We adjust the two QF and two QD in the dispersion suppressor to perfectly cancel the dispersion and its derivative. This slightly changes the beta functions and the phase advance across the arc. We will correct that later in the straight sections with additional matching quadrupoles. The left-hand plot in Figure 2 shows the dispersion suppressor and the plot on the right-hand side shows the dispersion across one arc. We observe that the dispersion suppressors at the entrance and exit of the arc—both having the same quadrupole excitations—nicely match the dispersion.

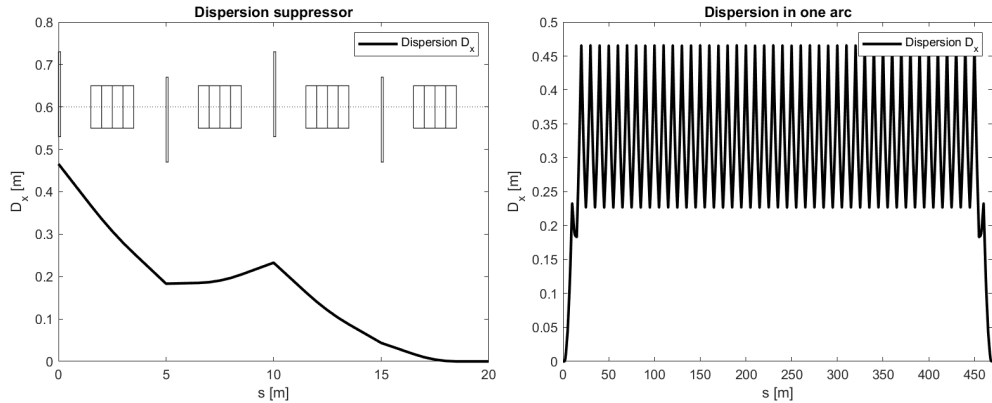


Figure 2: The horizontal dispersion function  $D_x$  in the dispersion suppressor (left) and the dispersion across one arc.

### 3 Straight sections

The two straight sections consist of six 90-degree cells as shown on the left-hand side in Figure 1. In one of the straight sections of the racetrack we use two central cells to adjust the tunes; the two QF and two QD are powered in series. Moreover the two adjacent cells on either side are used to match the beta functions to those of the arcs. We adjust the tunes to 26.413 in the horizontal plane and to 24.528 in the vertical plane and show the beta functions in this straight section in Figure 3. It turned out to be beneficial to have one tune below and the other above the half-integer, because the skew quadrupoles will push the fractional tunes apart. Conversely, if both are below the half-integer, one of them will cross the half-integer resonance, which leads to an unstable lattice.

The straight section on the other side of the ring also consists of six 90-degree FODO cells. With skew quadrupoles turned off, the transfer matrix of the straight section simply matches one arc to the next. In three of the six cells we place thin-lens skew quadrupoles in the middle of the drift space between a defocusing and a focusing quadrupole. They are shown by the red markers in the lattice at the bottom of both plots in Figure 4. At this location the value of both beta functions is equal to  $\beta_0 = 3L/2 = 7.5$  m and the phase advance between adjacent skew quadrupoles is  $90^\circ$  in both planes. If the focal length of the skew quadrupoles  $f_s$  is set to  $f_s = \beta_0$  the diagonal

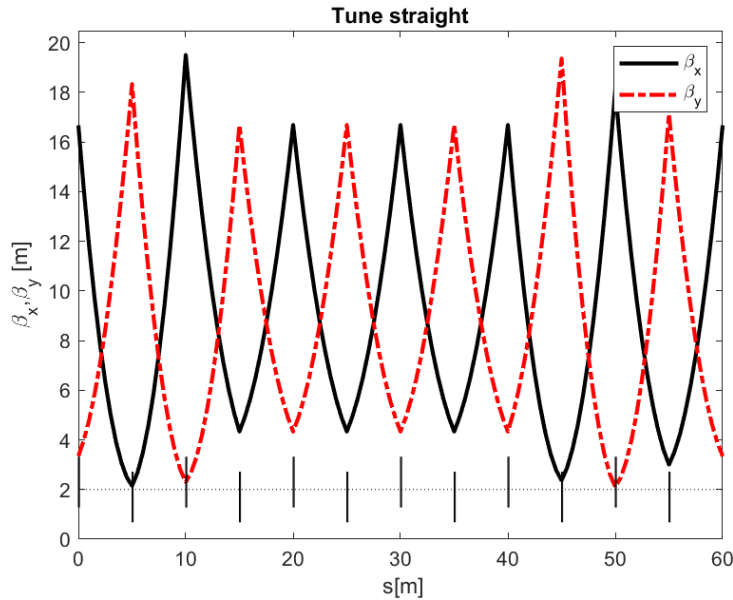


Figure 3: Beta functions in the straight section to adjust the tunes. The four quadrupoles in the two cells at the ends are used to match the beta functions to those of the arcs. The four quadrupoles in the middle are used to adjust the tunes.

$2 \times 2$  blocks of the transfer matrix for this section are zero, while the off-diagonal blocks are non-zero; it exchanges the transverse planes. Adjusting the excitations of the three skew quadrupoles by the same factor therefore allows us to continuously vary the coupling from the uncoupled configuration shown on the left-hand plot in Figure 4 to the Möbius configuration, shown on the right-hand plot.

## 4 The ring

The complete ring consists of the two straight sections sandwiched between the arcs starting with the Möbius straight. The upper plots in Figure 5 show the beta functions and the dispersions in the uncoupled configuration with skew quadrupoles turned off. The straight section with skew quadrupoles is located between  $s = 0$  and  $60$  m, where we observe the dispersions to be zero. The straight section to adjust the tunes is located between  $s = 500$  m and

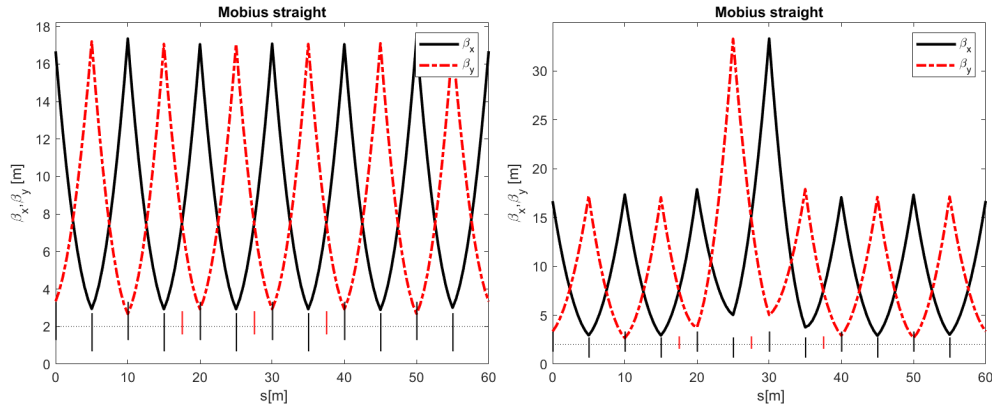


Figure 4: Beta functions in the straight section to adjust the coupling. On the left-hand side the skew quadrupoles are turned off and on the right-hand side they are turned on. The location of the skew quadrupoles is indicated by the red markers in the lattice shown near the bottom.

600 m, where the dispersion also is zero. In this configuration the tunes are  $Q_x = 26.413$  and  $Q_y = 24.528$ .

The middle plot in Figure 5 shows the beta functions for the fully-coupled configuration with focal length of the skew quadrupoles adjusted to  $f_s = \beta_0$ , which causes the two  $2 \times 2$  blocks on the diagonal of the transfer matrix for the whole ring to be zero while the off-diagonal  $2 \times 2$  blocks are non-zero. We calculate the shown beta functions and tunes in this strongly coupled lattice with the Edwards-Teng algorithm [7], refined by Sagan and Rubin [8]. In this configuration the tunes are  $Q_a = 26.220$  and  $Q_b = 24.720$ . Note that the fractional parts differ by a half-integer, a feature that we discuss further below. It is noteworthy that, apart from a moderate mismatch in the straight section with the skew quadrupoles, the beta functions are equal to those in the uncoupled configuration. A reason is that both straight sections are matched to the arcs and that the dispersion at the location of the skew quadrupoles is zero. In this way adjusting the coupling is independent of the rest of the optics.

The bottom plot in Figure 5 shows the beta functions for a configuration with focal length of the skew quadrupoles set to  $f_s = 2\beta_0$ , which causes significant beating of the beta functions in the arcs. We point out that the dispersions for all three configurations are the same as those shown in the

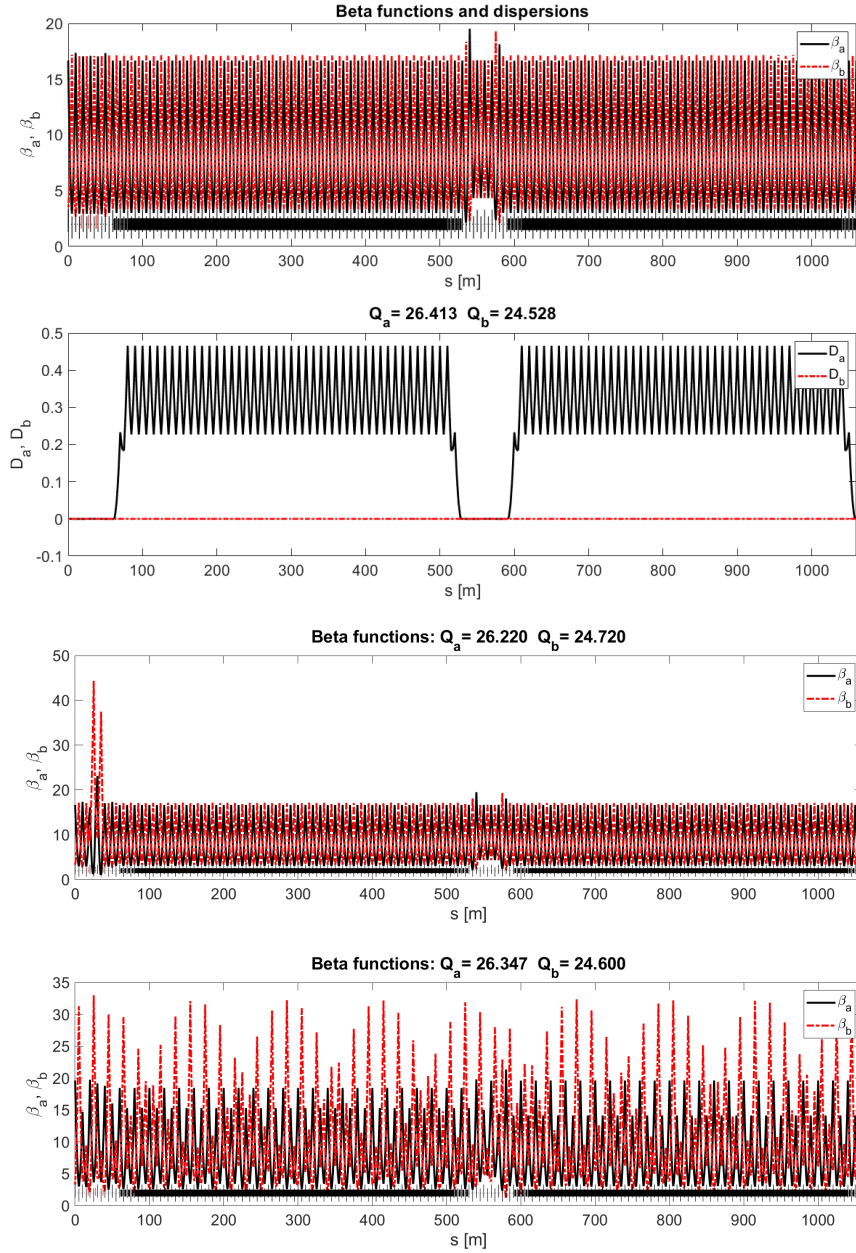


Figure 5: Beta functions and dispersion in the Möbius ring with skew quadrupoles turned off (top). The beta functions with skew quadrupoles turned on (middle), and set to a value half way in between (bottom).

Beam parameters	Beam parameters
$E_0 = 10 \text{ GeV}$ $C = 1060\text{m}$	$E_0 = 10 \text{ GeV}$ $C = 1060\text{m}$
$Q_a = 26.413$ $Q_b = 24.528$	$Q_a = 26.22$ $Q_b = 24.72$
$\text{eps}_a = 1.86\text{e-}08$ $\text{eps}_b = 0$	$\text{eps}_a = 9.29\text{e-}09$ $\text{eps}_b = 9.29\text{e-}09$
$\text{tau}_a = 9.19 \text{ ms}$ $\text{tau}_b = 9.17 \text{ ms}$	$\text{tau}_a = 9.18 \text{ ms}$ $\text{tau}_b = 9.18 \text{ ms}$
$\text{tau}_e = 4.58 \text{ ms}$ $\text{sig}_p = 7.99\text{e-}04$	$\text{tau}_e = 4.58 \text{ ms}$ $\text{sig}_p = 7.99\text{e-}04$
$\text{alpha} = 1.88\text{e-}03$	$\text{alpha} = 1.88\text{e-}03$
$I_1 = 1.998$ $I_2 = 0.05476$ $I_3 = 0.00047787$	$I_1 = 1.998$ $I_2 = 0.05476$ $I_3 = 0.00047787$
$I_{4a} = 0.000152$ $I_{4b} = 0$	$I_{4a} = 7.61\text{e-}05$ $I_{4b} = 7.61\text{e-}05$
$I_{5a} = 6.92\text{e-}06$ $I_{5b} = 0$	$I_{5a} = 3.46\text{e-}06$ $I_{5b} = 3.46\text{e-}06$

Figure 6: Beam parameters for the uncoupled configuration (left) and the Möbius configuration (right).

uncoupled configuration.

We now turn to the calculation of the beam parameters as we increase the excitation of the skew quadrupoles.

## 5 Beam parameters

We now calculate the beam parameters using the algorithm described in [1]. Those corresponding to the configurations for the uncoupled and the Möbius ring that gave rise to the upper and middle plots in Figure 5 are shown in Figure 6. We observe that the emittances for the uncoupled lattice are 18.6 nm-rad and zero, whereas for the Möbius configuration both emittances are 9.3 nm-rad. We also find that the small differences in the transverse damping times of the uncoupled configuration vanishes in the Möbius configuration. The longitudinal parameters for both configurations are equal. In the rows below we show the radiation integrals. Only  $I_{4a}$  and  $I_{4b}$  as well as  $I_{5a}$  and  $I_{5b}$  differ between the configurations, where the corresponding values in the Möbius configuration are equal to half the horizontal values  $I_{4a}$  and  $I_{5a}$  of the uncoupled configuration. In the Möbius configuration, the effect of damping and excitation is shared equally between the two planes.

Since only the tunes and emittances show a significant difference between the two configurations, we explore their variation further as we increase the strength of the skew quadrupoles. On the upper panel in Figure 7 we show the change of the fractional tunes. We observe that the increasing skew quadrupoles “push the fractional tunes apart.” Note, however, that the

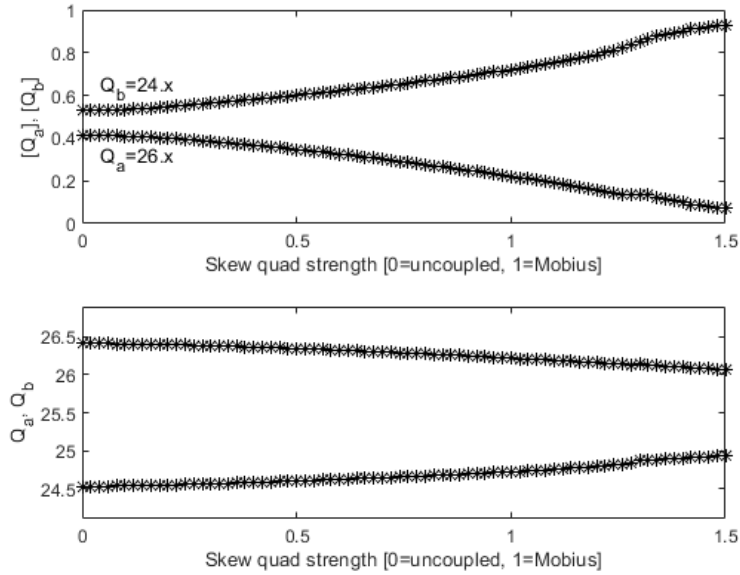


Figure 7: The fractional tunes (top) and the full tunes (bottom) as a function of the excitation of the skew quadrupoles.

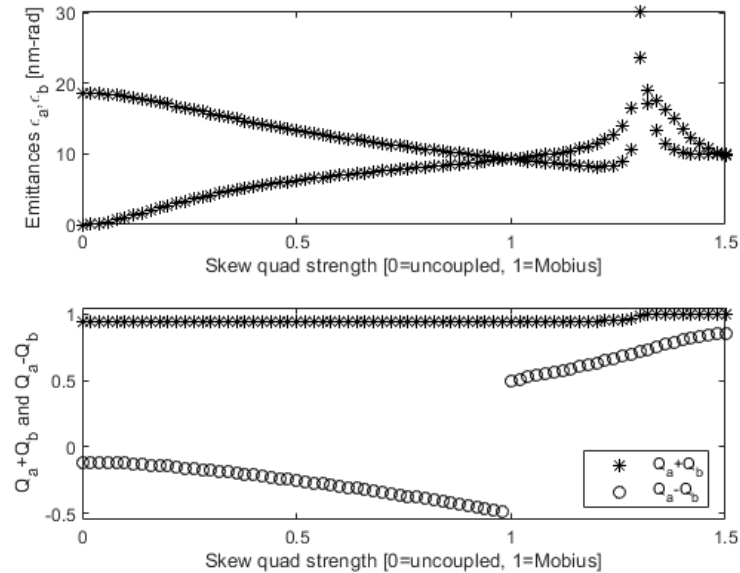


Figure 8: The emittances (top) and the difference and sum of the fractional tunes (bottom) as a function of the excitation of the skew quadrupoles.



upper branch corresponds to the “vertical” tune  $Q_b$  and the lower branch to the “horizontal” tune  $Q_a$ . The lower panel also shows both tunes but including their integral part.

The upper panel in Figure 8 shows the emittances as a function of the excitation of the skew quadrupoles. We see that initially  $\varepsilon_a$  is non-zero and  $\varepsilon_b$  is zero, but as the coupling increases their values get closer and become equal in the Möbius configuration. This is accompanied by the difference of the fractional tunes approaching a half-integer. This is apparent from the circles on the lower panel, which show  $Q_a - Q_b$ . If we increase the excitation beyond the Möbius configuration both emittances increase dramatically. The plot on the lower panel provides an explanation; the sum of the tunes  $Q_a + Q_b$  becomes an integer and the system crosses a sum resonance shown by the asterisks in the lower panel from Figure 8. And on a sum resonance, the emittances can become arbitrarily large, because only their difference is bounded [9, 10].

## 6 Conclusions

In order to explore the ability of the new method to calculate synchrotron radiation integrals [1] to handle highly-coupled systems we designed a ring, based on 90-degree FODO cells, which can be continuously tuned from an uncoupled to a Möbius configuration. The method works well and allow us to calculate all beam parameters that depend on the synchrotron radiation integrals. In particular, the damping times only show a small dependence on the coupling whereas the emittances, which differ greatly in the uncoupled configuration, become equal in the Möbius configuration. If we increase the coupling beyond the Möbius configuration, the system encounters a sum resonance, where both emittances grow significantly, consistent with [9, 10].

Having the emittances and momentum spread available, we can calculate the self-consistent equilibrium beam sizes in all three dimensions, even for highly-coupled lattices.

Apart from serving as a test ground for the new method to calculate synchrotron radiation integrals, the Möbius ring might become useful to explore the effect of coupling on orbit correction, non-linear effects, and the beam-beam interaction.

## References

- [1] V. Ziemann, A. Streun, *Equilibrium parameters in coupled storage ring lattices and practical applications*, in preparation.
- [2] Richard H. Helm, Martin J. Lee, P. L. Morton, and M. Sands, *Evaluation of synchrotron radiation integrals*, IEEE Trans. Nucl. Sci. 20 (1973) 900.
- [3] R. Talman, *A proposed Möbius accelerator*, Physical Review Letters 74 (1995) 1590.
- [4] Software used to design the Möbius ring is available from <https://github.com/volkziem/MobiusRing>.
- [5] V. Ziemann, *Hands-On Accelerator Physics Using MATLAB*, CRC Press, Boca Raton, 2019.
- [6] M. Aiba, M. Ehrlichman, A. Streun, *Round beam operation in electron storage rings and generalization of Möbius accelerator*, Proceedings of IPAC 2015 in Richmond VA, USA, (2015) 1716.
- [7] D. Edwards, L. Teng, *Parameterization of linear coupled motion in periodic systems*, IEEE Trans. Nucl. Sci. 20 (1973) 885.
- [8] D. Sagan and D. Rubin, *Linear analysis of coupled lattices*, Phys. Rev. ST Accel. Beams, 2:074001, 1999. [Phys. Rev. ST Accel. Beams3,059901(2000)].
- [9] Section 1.3.1 in H. Wiedemann, *Particle Accelerator Physics II, 2nd ed.*, Springer Verlag, Heidelberg, 2003.
- [10] Section 2.1.3 in A. Chao, M. Tigner, *Handbook of Accelerator Physics and Engineering*, World Scientific, Singapore, 1999.